Polym. Bull. (2017) 74:517–529
DOI 10.1007/s00289-016-1727-y

ORIGINAL PAPER

Preparation and characterization of polyurethane/POSS hybrid aqueous dispersions from mono-amino substituted POSS

Tonghui Hao[1] · Xiaoyang Liu[1] · Guo-Hua Hu[2] · Tao Jiang[1] · Qunchao Zhang[1]

Received: 17 November 2015 / Revised: 10 April 2016 / Accepted: 16 June 2016 /
Published online: 22 June 2016

Abstract A series of linear polyurethane (PU) aqueous dispersions modified by polyhedral oligomeric silsesquioxane (POSS) was synthesized by incorporating various amounts (ca. 2–10 wt%) of a secondary amino-terminated monofunctional POSS in hexamethylene diisocyanate trimer (HDI-T), hexamethylene diisocyanate, poly(tetramethylene-oxide) and 2,2-bis(hydroxymethyl)propionic acid. Results from the gel permeation chromatography, Fourier-transform infrared spectroscopy, transmission electron microscopy, and X-ray diffraction showed that the POSS monomers could be effectively introduced into the PU matrices based on HDI-T to obtain stable aqueous and homogenous PU/POSS hybrid dispersions. The thermal properties of the hybrids do not significantly affect the degradation mechanism of the PU. The physical properties of the PU/POSS hybrid films changed, with a notable increase in tensile strength and surface hydrophobicity.

Keywords Aqueous polyurethane dispersions · POSS · Hexamethylene diisocyanate trimer · Hydrophobicity

Introduction

The incorporation of inorganic or organometallic segments into polymers has been intensively investigated to develop new materials with enhanced properties [1–6]. Composites made of graphite oxide (m-GO), multi-walled carbon nanotubes

✉ Qunchao Zhang
zhangqc1976@hubu.edu.cn

[1] Hubei Collaborative Innovation Center for Advanced Organic Chemical Materials, Hubei University, Wuhan 430062, China

[2] Laboratory of Reactions and Process Engineering (LRGP), CNRS-University of Lorraine, 1 rue Grandville, BP 20451, 54001 Nancy Cedex, France

(MWCNTs) etc. nano sized particles and polymers are widely believed to offer the potential for the design of novel or at least improved materials [7–21].

Contrary to conventional inorganic fillers, polyhedral oligomeric silsesquioxanes (POSS), with fascinating structures and unique properties, are emerging as a new chemical technology for nano reinforced organic–inorganic hybrids. Many studies have focused on POSS-modified polymers because of the simplicity of their processing; these polymers also possess excellent comprehensive properties as comonomers and cross-linkers for polystyrene, nylon, epoxy, cellulose, polycarbonate, polyacrylate, urethane–urea, imide, siloxane, and other polymer matrices [22]. Various copolymers and networks usually display enhanced viscoelasticity, mechanical properties, high thermal stability, oxygen permeability, low thermal conductivity, thermal expansion, dielectric permittivity [23], and surface energy [24]. Thus, these nanocomposites containing POSS units have been extensively applied as coatings [25], components in catalysis [26], and drug delivery systems [27].

The covalent incorporation of reactive POSS monomers into polyurethanes (PUs), such as diamino or diol-functionalized POSS, via copolymerization, grafting, and blending processes has recently been received much attention [28–32]. However, Environmental concerns press for the development of eco-friendly materials. For example, aqueous polyurethane (PU) dispersions are replacing solvent-based ones. Most aqueous PU dispersions are linear polyurethanes with polar groups in the main chain. Their mechanical properties and solvent resistance are inferior to those of solvent-based ones. Recent studies report on the incorporation of polyhedral oligomeric silsesquioxane (POSS) to improve properties of aqueous PU dispersions [33–38].

This work aims at developing a new method of incorporating POSS to PU matrices to prepare aqueous PU dispersions with improved properties. The synthesis route of aqueous PU dispersions is depicted in Scheme 1. It is composed of four steps [39, 40]. Step 1 consists in reacting hexamethylene diisocyanate trimer (HDI-T) with *N*-(*n*-butyl)-3-aminopropyl-heptaisobutyl-POSS (APS, mono-amino substituted POSS) to form a POSS bearing diisocyanate. In step 2, the POSS bearing diisocyanate together with hexamethylene diisocyanate (HDI) reacts a mixture of two diols, 2,2-bis(hydroxymethyl) propionic acid (DMPA) and poly(tetramethylene oxide) (PTMO, $M_n = 2000$) to obtain a POSS bearing polyurethane prepolymer which still contains two terminal isocyanate groups. In step 3, the chains of the POSS bearing polyurethane prepolymer is extended using 1,4-butanediol (BD) as a chain extender. The resulting product is then neutralized with triethylamine (TEA). Step 4 (the last step) is to add water in and to evaporate tetrahydrofuran (THF) to obtain aqueous PU/POSS hybrid dispersions. The originality of the synthesis route developed in this work lies in step 1, namely, the reaction between HDI-T and APS (mono-amino substituted POSS). This allows obtaining a POSS bearing diisocyanate, an intermediate for the subsequent synthesis of PU/POSS hybrid dispersions.

The structures and morphologies of the aqueous PU/POSS hybrid dispersions are investigated using gel permeation chromatography (GPC), Fourier-transform infrared (FTIR) spectroscopy, transmission electron microscopy (TEM), and

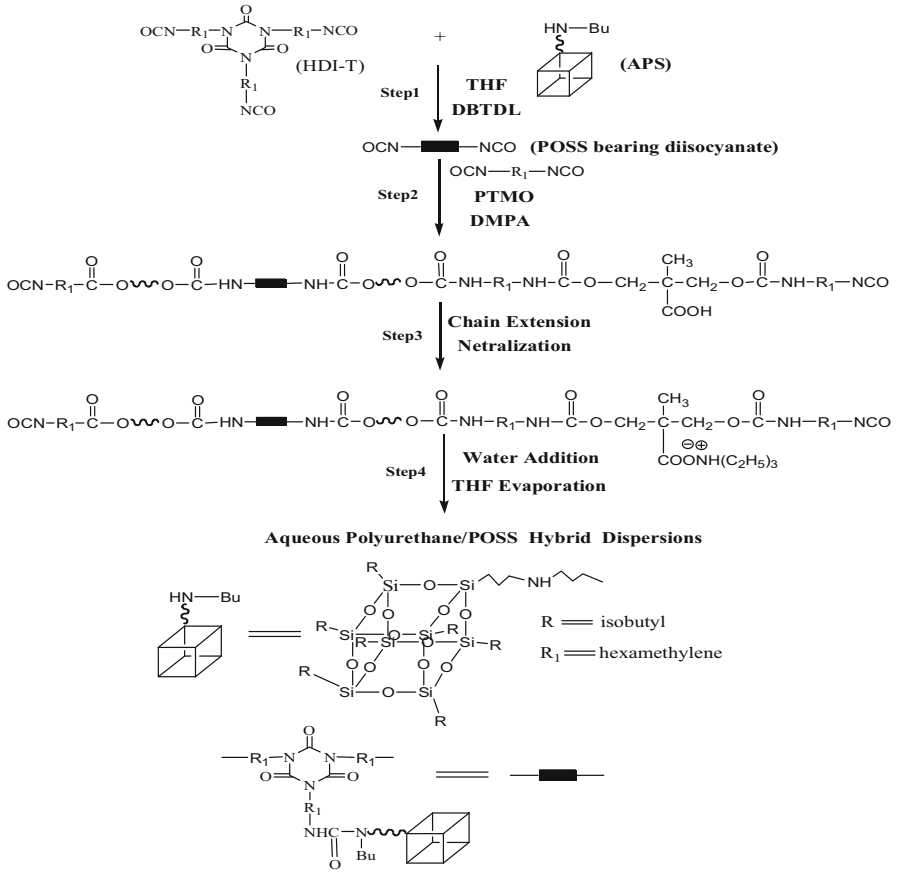

Scheme 1 Synthesis route of aqueous PU/POSS hybrid dispersions

X-ray diffraction (XRD). Their mechanical, thermal, and hydrophobic properties are characterized by dynamic mechanical analysis, tensile testing, thermal gravimetrical analysis (TGA), and static contact angle measurement.

Experimental

Materials

Hexamethylene diisocyanate (HDI), hexamethylene diisocyanate trimer (HDI-T, Desmodur N-3300, –NCO % = 21.26 tested), 2,2-bis(hydroxymethyl) propionic acid (DMPA) and poly(tetramethylene oxide) (PTMO, $M_n = 2000$) were purchased from Bayer Material Science (Pittsburgh, PA). *N*-(*n*-Butyl)-3-aminopropyltriethoxy-silane (BAPTS) was provided by Hubei Diamond Advanced Material of Chemical Inc. (Hubei, China). Trisilanolisobutyl-POSS was obtained from Hybrid

Plastics. *N*-(*n*-Butyl)-3-aminopropyl-heptaisobutyl-POSS, dibutyltin dilaurate (DBTDL), triethylamine (TEA), 1,4-butanediol (BD), acetone, butylol (But-4), ethanol, tetraethylammonium hydroxide and tetrahydrofuran (THF) were received from Shanghai Regent Chemical Co. (Shanghai, China).

Synthesis of the *N*-(*n*-butyl)-3-aminopropyl-heptaisobutyl-POSS (APS)

Trisilanolisobutyl POSS (79.1 g, 0.10 mol) was dissolved in ethanol (500 ml) followed by the addition of BAPTS (27.7 g, 0.10 mol) and tetraethylammonium hydroxide (1.2 g, 2.04 mM of a 25 % methanol solution). The clear solution was stirred at 20 °C for 36 h. The solvent was evaporated and the product was washed with acetonitrile, and then dried to yield 87 g of white solid (yield 94 %). ^{1}H NMR (ppm) (300 MHz, $CDCl_3$): δ2.60 (m, 4H, CH_2), 1.85 (m, 7H, –CH–), 1.58 (m, 2H, CH_2), 1.47 (m, 2H, CH_2), 1.35 (m, 2H, CH_2), 0.95 (m, 9H, CH_3), 0.60 (t, 2H, CH_2), 0.52(t, 2H, CH_2). ^{13}C NMR (ppm) (300 MHz, $CDCl_3$): δ52.36 (s, CH_2), 49.34 (s, CH_2), 32.12 (s, CH_2), 25.59 (s, CH_3), 23.76 (s, –CH–), 22.93 (s, CH_2), 22.36 (s, CH_2), 20.44 (s, CH_2), 13.94 (s, CH_3), 9.54 (s, CH_2). ^{29}Si NMR (ppm) (300 MHz, $CDCl_3$): δ-66.88, −67.07. ESI–MS: $m/z = 930$, $[M+H]^+$, 100 %.

Preparation of POSS modified aqueous polyurethane dispersions (PU/POSS)

A series of PU/POSS was synthesized in a round-bottom flask equipped with a mechanical stirrer (600 rpm), a nitrogen inlet and a condenser. A water bath was employed to fix the reaction temperature. The preparation of the aqueous PU/POSS hybrids was composed of four main steps:

1. Synthesis of a POSS bearing diisocyanate by reacting HDI-T with APS.
2. Synthesis of a POSS bearing polyurethane prepolymer by reacting the POSS bearing diisocyanate and HDI with a mixture of two different diols, DMPA + PTMO.
3. Chain extension of the POSS bearing polyurethane prepolymer with BD and then neutralization of the resulting product with a tertiary amine (TEA).
4. Emulsification to obtain aqueous PU/POSS hybrid dispersions. In this step, water was added in the system and the solvent was evaporated from therein.

More specifically, APS and HDI-T were added in a 250 ml round-bottom flask with anhydrous THF and DBTDL (a catalyst) at room temperature and under stirring over a period of 12 h. HDI, PTMO and DMPA were sequentially fed in under stirring and the reaction temperature was raised to 60 °C. After 3 h of reaction, the resulting prepolymer was chain extended with BD and the reaction continued for another 2 h so that it could go to completion. Finally, the polymer was neutralized by the addition of triethylamine under stirring at 60 °C for 30 min.

After the neutralization of the PU/POSS, the flask was maintained at 60 °C but the mechanical stirring speed was raised to 1300 rpm to promote its dispersion in water. Water was added dropwise to the flask and the system was stirred for

additional 30 min. Finally, THF was removed from the system using a rotary evaporator. The solid content of the resulting dispersion was about 30 wt%.

Characterizations

The molecular weights of the PU and PU/POSS samples were determined by GPC measurements in THF (Waters, GPCV-2000). The calibration was based on polystyrene standards (M_n = 178,700, 50,100, 9400 and 3060, respectively).

Infrared spectra were recorded on a FT-IR spectrometer (170SX, Nicolet, USA) in the transmission mode at room temperature from 4000 to 600 cm^{-1} with a resolution of 2 cm^{-1} and an accumulation of 16 scans. Each of the samples was coated on a KBr disk.

The size distribution of the PU/POSS dispersions was measured using a Zetasizer Nano ZS (Malvern Instruments Ltd., UK) equipment. The viscosity of the dispersions was measured with a Brookfield LVDV-II viscometer (Middleboro, MA) at 25 °C. The dispersions in sealed bottles were kept at room temperature to evaluate the storage stability.

TEM observation of the PU10 was carried out on a JEM-2010 FEF (UHR) transmission electron microscope (JEOL, Japan).

XRD patterns were recorded on a D/Max-IIIA X-ray diffractormeter (Rigaku Denki, Japan) using Cu Kα radiation source (λ = 0.154 nm) at 40 kV and 60 mA with a scan rate of 5°/min. The diffraction angle of 2θ ranged from 8° to 50°.

The DMA of the films prepared from the PU-POSS dispersions was carried out on a TA Instruments DMA Q800 dynamic mechanical analyzer in single cantilever mode at a frequency of 1 Hz and a heating rate of 5 °C/min, ranging from −100 °C to +100 °C.

The tensile strength at break (σ_b) and elongation at break (ε_b) of the PU/POSS dispersion-cast films were measured on a CMT6503 Universal Testing Machine (SANS, Shenzhen, China) at a crosshead rate of 100 mm/min according to ISOll84-1983.

A Perkin-Elmer thermal gravimetric analyzer (TGA-7) was used to investigate the thermal stability of the PU/POSS hybrids. The samples (about 10 mg) were heated under a nitrogen atmosphere from ambient temperature to 600 °C with a heating rate of 5 °C/min.

The contact angle of distilled, deionized water on the PU/POSS films was determined using a KRUSS DSA-100 contact angle meter. Three independent measurements were carried out, and the average contact angle was reported.

Results and discussion

Synthesis of PU/POSS hybrids

Table 1 shows the recipes for the synthesis of PU/POSS hybrids and the molecular weights of the resulting PUs. The POSS content is 0, 2, 6, 10 and 0 wt% named PU0, PU2, PU6, PU10 and PU10C, respectively. The molecular weights of the PU/

Table 1 Recipes for the synthesis of PU and PU/POSS hybrids

Sample	HDI-T[a] (mol)	POSS (mol)	But-4 (mol)	HDI (mol)	PTMO (mol)	DMBA (mol)	BD (mol)	M_n[b] (g/mol)	PDI[c]
PU0[d]	–	–	–	1.96	0.66	0.57	0.53	24,700	3.3
PU2	0.06	0.02	–	1.92	0.66	0.57	0.53	15,100	3.7
PU6	0.19	0.06	–	1.86	0.66	0.57	0.55	14,000	3.8
PU10	0.32	0.10	–	1.65	0.55	0.57	0.57	11,900	3.9
PU10C[e]	0.23	–	0.08	1.91	0.73	0.57	0.57	25,400	3.5

[a] –NCO = 21.26 wt%; [b] number-average molecular weight; [c] polydispersity index. [d] PU0 is a linear PU obtained without POSS nor HDI-T; [e] PU10C is another PU obtained without POSS but with HDI-T bearing diisocyanate by reacting HDI-T with butylol (But-4). Molar concentrations of all the above reactants are based on isocyanate equivalent, secondary amine equivalent or hydroxyl equivalent. For all recipes, the molar ratios of the total isocyanate is 1.12

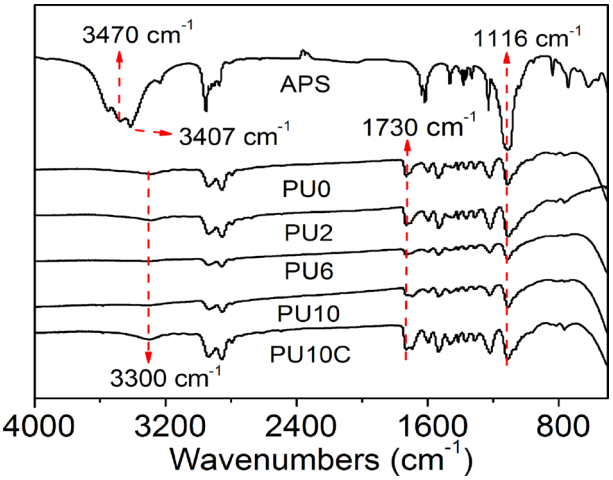

Fig. 1 FT-IR spectra of the POSS, PU and PU/POSS hybrids

POSS hybrids were much lower than those of PU10C and PU0. Moreover, they decrease slightly with increasing POSS content. Their polydispersity indexes are relatively close, from 3.3 to 3.9.

Structures of POSS-modified PU hybrids

Figure 1 shows the FTIR spectra of the POSS (APS), PU0 and PU/POSS hybrids [18, 19]. The formation of urethane moieties for the PU and PU/POSS hybrids is confirmed by the complete disappearance of the stretching vibration of the isocyanate at 2260 cm^{-1}, the appearance of the bending and stretching bands of the urethane amide at 1537 and 3330 cm^{-1} and the vibrating band of the carbonyl group at 1730 cm^{-1}. In the case of the POSS, the double bands at 3470 and 3407 cm^{-1} are typical of the secondary amine. The strong absorptions at 1116 and 836 cm^{-1}

correspond to the Si–O–Si asymmetric and symmetric stretching in the silsesquioxane cages. However, PU0 and PU10C also show a peak at 1116 cm^{-1}. The absorption region from 2860 to 2940 cm^{-1} corresponds to the $–CH_3$ stretching. The N–H of urethane are shown in the region from 1530 to 1663 cm^{-1}.

Figure 2 shows the TEM micrographs of PU0 and PU10 coating cross-linked films which have been stained by ruthenium tetroxide (RuO_4). The dark area or the very small dark particles could be assigned to the hard segment domains, whereas the bright region to the soft segment ones [41]. Compared with PU0 which does not contain any POSS, PU10 does not show any segregation or aggregation of POSS particles, exhibiting a finer structure. This tends to suggest that the POSS that is chemically linked to the hard segments of the PU improves the compatibility between hard and soft segments. This phenomenon is ascribed to the large surface area of nano-particles that create the large interaction domains with the PU hard and soft segments [42–44].

Figure 3 shows the XRD patterns of APS (the POSS), PU0 and PU2 to PU10 (the PU/POSS hybrids films). PU0 shows two sharp reflections at $2\theta = 19.8°$ and 24.2°, which correspond to the PTMO crystal [28]. The pure POSS monomer shows three sharp peaks at11°, 12.2°, and 19.2°, which is in line with Ref. [33], especially the most intense one at 8.3° indexed as 101. PU2 to PU10 (PU/POSS hybrids films) do not show any reflections corresponding to the crystalline POSS, indicating that the POSS moieties which are chemically linked to the PU chain are unable to crystalline. On the other hand, PU0 to PU6 show sharp peaks around 19.8° and 24.2°. These two peaks have disappeared in the case of PU10C and PU10. PU10C was obtained more cross-linked densities than PU0 to PU6 duo to react by HDI-T and BD. However, PU10 whose POSS content is the highest (10 wt%) indicating that when the content of the POSS linked to the PU reaches a certain threshold. The soft segments of PU10 and PU10C crystallize in a much more difficult manner. Consequently, the compatibility between the soft and hard segments of the PU is improved. These findings are consistent with the formation of POSS nanocrystals in

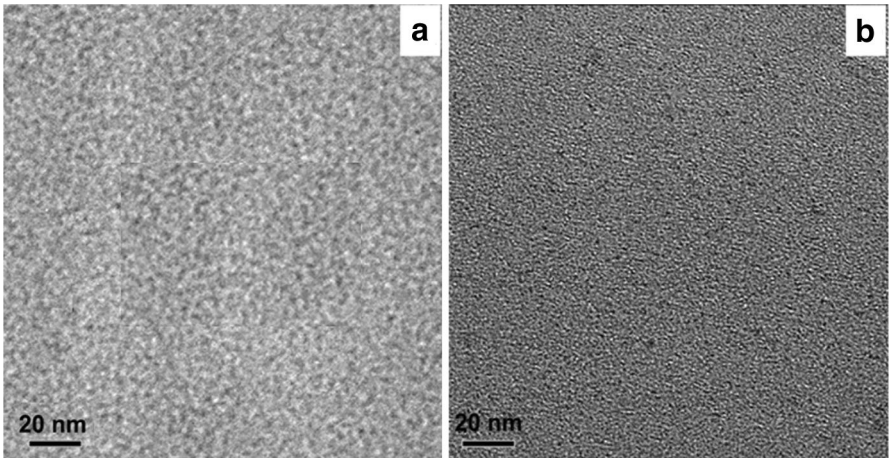

Fig. 2 TEM micrograph of **a** PU0 and **b** PU10 (PU/POSS) hybrids films

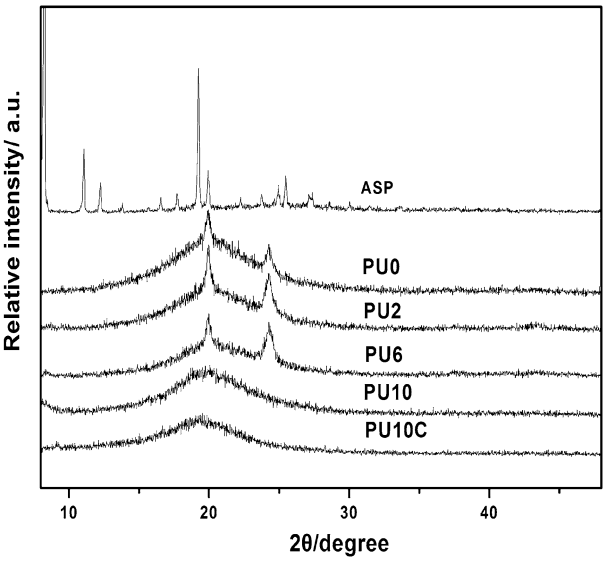

Fig. 3 XRD profiles of PU0, the POSS and PU/POSS hybrids and PU10C

Table 2 Physical properties of the PU and PU/POSS hybrids

Sample code	PU0	PU2	PU6	PU10	PU10C
Viscosity (mPa·s)	67	65	64	66	70
Particle diameter (nm)	114	109	115	120	116

the PU hard segments (especially at high POSS concentrations) as reported in the literature [19, 28]. They are also in good agreement with the TEM results [41] (Fig. 2).

Particle size and viscosity of the PU/POSS hybrid dispersions

Table 2 shows the viscosity and particle diameter of PU and different PU/POSS hybrid dispersions (they all contain 30 wt% solids). The viscosity and particle diameter are very similar for all dispersions from PU0 to PU10C. The viscosity is from 64 to 70 mPa·s and the particle diameter is from 109 to 120 nm. This shows that the dispersion process is not greatly affected by the incorporation of the POSS into the PU.

Mechanical properties

Figure 4a, b shows the temperature dependence of the storage modulus (E') and the loss peak (tanδ) of the PU0, PU10C and PU/POSS hybrid films, respectively. The E' values of all PU/POSS hybrids (PU2, PU6 and PU10) are significantly higher than those of PU0 and PU10C. Moreover, E' increases significantly with increasing

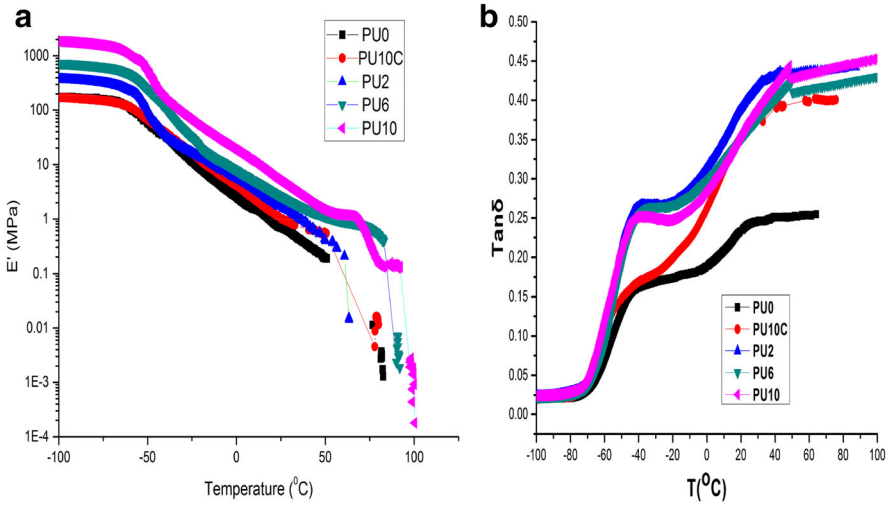

Fig. 4 Temperature dependence of **a** the storage modulus (E'); **b** the loss peak (tanδ) for the PU/POSS hybrids, PU0 and PU10C

POSS content. These indicate that the presence of nano-scale POSS cages in the PU increases the modulus of the latter [19, 41].

From Fig. 4b, all tanδ curves of the PU/POSS hybrids show a single peak around −40 °C were glass transition temperature (T_g) of soft segments (PTMO). The similar T_g indicating that the POSS is homogeneously distributed in the PU matrix. This is also consistent with the TEM results. Meanwhile, compared with PU0 and PU10C, the values of tanδ of the POSS/PU hybrids increases with increasing POSS content from 0.15 to 0.25. It should be pointed out that the presence of POSS may affect motion of polymer chains of polymers in at least three different ways. First, the dispersion of POSS cages at the molecular level could restrict the motion of polymer chains, which would decrease tanδ; second, the inclusion of bulky POSS moieties increases the free volume of the polymer system, which would increase tanδ; and third, the inclusion of POSS cages could act as a plasticizer by reducing interactions such as hydrogen bonding between polymer chains, which could increase tanδ. From Fig. 4b, the tanδ peaks gradually broadens and their heights increase with increasing POSS content, the motion of soft segments would affect composites' crystallization, this is consistent with the XRD results.

Table 3 shows the tensile strength at break and elongation at break of the PU and PU/POSS hybrid films. The tensile strength at break increases with increasing POSS content while the elongation at break decreases accordingly. POSS reinforced films resulting from the POSS has played the role of the cross links to form increased network structure [19, 20].

Thermal properties

Figure 5 shows the TGA curves of the PU and PU/POSS hybrid films. All samples follow a similar degradation trend, suggesting that the presence of POSS does not significantly affect the degradation mechanism of the PU [25, 45–47].

Table 3 Mechanical properties of the PU and PU/POSS hybrids

Sample code	PU0	PU2	PU6	PU10	PU10C
Tensile strength at break (MPa)	1.21	2.24	6.20	12.40	1.46
Elongation at break (%)	1700	1400	1100	800	1500

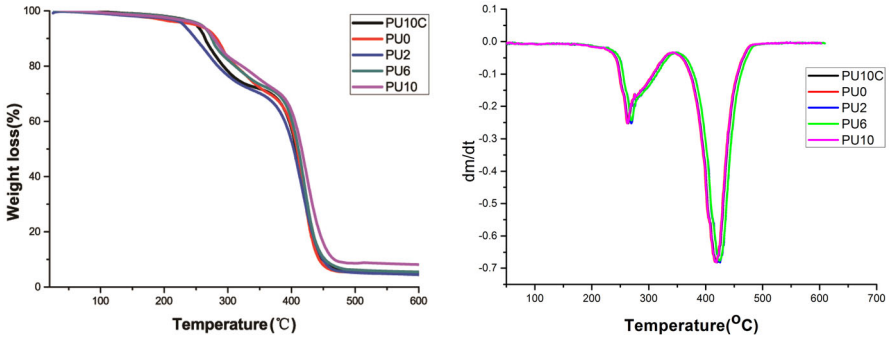

Fig. 5 TGA curves of the PU and PU/POSS hybrids

Hydrophobic properties

The contact angle with water, which characterizes the hydrophobicity of the PU and PU/POSS hybrids films, is 65°, 86°, 93°, 99° and 69° for PU0, PU2, PU6, PU10 and PU10C, respectively. The PU0 and PU10C which do not contain any POSS are relatively hydrophobic as their contact angles are 65° and 69°, respectively. The incorporation of the POSS improves the hydrophobicity of the PU. Moreover, the hydrophobicity of the PU/POSS increases with increasing POSS content, reading 99° when the POSS content is 10 wt% (Fig. 6).

Conclusions

We have successfully fabricated polyurethane (PU)/POSS hybrid dispersions by incorporating secondary amino-terminated functional POSS into PU matrices based on hexamethylene diisocyanate trimer (HDI-T) to partly substitute hexamethylene diisocyanate (HDI). The results show that water dispensability of the PU is not affected by the incorporation of the reactive POSS with a mono-secondary-amino-terminated structure (up to 10 %), and that the POSS is homogeneously dispersed in the PU matrix. The presence of POSS does not significantly affect the degradation mechanism of the PU. However, the E' and tanδ values of all PU/POSS hybrids (PU2, PU6 and PU10) are significantly higher than those of PU0 and PU10C. Moreover, E' and tanδ increases significantly with increasing POSS content. Meanwhile the tensile strength at break increases from 1.21 to 12.4 MPa with increasing POSS content from 0 to 10 wt% while the elongation at break decreases

Fig. 6 The contact angle of **a** PU0, **b** PU10C, **c** PU2, **d** PU6 and **e** PU10

from 1700 to 800 % accordingly. The PU/POSS hybrids not only exhibit good mechanical strength, but also bring about significant improvement in hydrophobicity.

References

1. Chen M, Zhou SX, You B, Wu LM (2005) A novel preparation method of Raspberry-like PMMA/SiO2 hybrid microspheres. Macromolecules 38:6411–6417
2. Yeh JM, Liou SJ, Lin CY, Cheng CY, Chang YW (2002) Anticorrosively enhanced PMMA−clay nanocomposite materials with quaternary alkylphosphonium salt as an intercalating agent. Chem Mater 14:154–161
3. Xiong M, You B, Zhou SX, Wu LM (2004) Study on acrylic resin/titania organic–inorganic hybrid materials prepared by the sol–gel process. Polymer 45:2967–2976
4. Lee H, Archer LA (2001) Functionalizing polymer surfaces by field-induced migration of copolymer additives. 1. Role of surface energy gradients. Macromolecules 34:4572–4579
5. Yuan JJ, Zhou SX, Wu LM, You B (2006) Organic pigment particles coated with titania via sol−gel process. J Phys Chem B 110:388–394
6. Li YQ, Fu SY, Mai YW (2006) Preparation and characterization of transparent ZnO/epoxy nanocomposites with high-UV shielding efficiency. Polymer 47:2127–2132
7. Zeng F, Feng G, Son TN, Hai MD (2015) Advanced multifunctional graphene aerogel—Poly (methyl methacrylate) composites: experiments and modeling. Carbon 81:396–404
8. Mahbub H, Kakarla RR, Enamul H, Andrew IM, Vincent GG (2013) High-yield aqueous phase exfoliation of graphene for facile nanocomposite synthesis via emulsion polymerization. J Colloid Interface Sci 410:43–51
9. Su JH, Hyung L, Han MJ, Byung KK, Anjanapure VR, Kakarla RR (2014) Graphene modified lipophilically by stearic acid and its composite with low density polyethylene. J Macromol Sci Part B Phys 53:1193–1204
10. Kakarla RR, Mahbub H, Vincent GG (2015) Hybrid nanostructures based on titanium dioxide for enhanced photocatalysis. Appl Catal A Gen 489:1–16
11. Kakarla RR, Byung CS, Kwang SR, Jin CK, Hoeil C, Youngil L (2009) Conducting polymer functionalized multiwalled carbon nanotubes with noble metal nanoparticles: synthesis, morphological characteristics and electrical properties. Synth Met 159:595–603
12. Mahbub H, Kakarla RR, Enamul H, Shaikh NF, Samira G, Andrew IM, Vincent GG (2014) Hierarchical assembly of graphene/polyaniline nanostructures to synthesize free-standing supercapacitor electrode. Compos Sci Technol 98:1–8
13. Kakarla RR, Kwang-Pill L, Anantha IG, Ali MS (2007) Synthesis and properties of magnetite/poly (aniline-co-8-amino-2-naphthalenesulfonic acid) (SPAN) nanocomposites. Polym Adv Technol 18:38–43
14. Kakarla RR, Kwang-Pill L, Anantha IG (2007) Self-assembly directed synthesis of poly(ortho-toluidine)-metal(gold and palladium) composite nanospheres. J Nanosci Nanotechnol 7:3117–3125
15. Yu RL, Soon CK, Hyung-il L, Han MJ, Anjanapura VR, Kakarla RR, Byung KK (2011) Graphite oxides as effective fire retardants of epoxy resin. Macromol Res 19:66–71
16. Kakarla RR, Han MJ, Youngil L, Anjanapura VR (2010) Synthesis of MWCNTs-core/thiophene polymer-sheath composite nanocables by a cationic surfactant-assisted chemical oxidative polymerization and their structural properties. Polym Sci Part A Polym Chem 48:1477–1484

17. Zhang YP, Lee SH, Kakarla RR, Anantha IG, Kwang-Pill L (2007) Synthesis and characterization of core-shell SiO_2, nanoparticles/poly(3-aminophenylboronic acid) composites. J Appl Polym Sci 104:2743–2750
18. Kakarla RR, Anjanapura VR, Han MJ, Siddaramaiah (2009) Synthesis and characterization of pyridine-based polyurethanes. Des Monomers Polym 12:109–118
19. Kakarla RR, Anjanapura VR, Han MJ (2008) Synthesis and characterization of novel polyurethanes based on 4,4'-{1,4-phenylenebis[methylylidenenitrilo]diphenol. Polym Bull 60:609–616
20. Sang HC, Dong HK, Anjanapura VR, Kakarla RR, Hyung IL, Koo SY, Han MJ, Byung KK (2012) Properties of graphene/waterborne polyurethane nanocomposites cast from colloidal dispersion mixtures. J Macromol Sci Part B Phys 51:197–207
21. Orgilés-Calpena E, Arán-Aís F, Torró-Palau AM, Orgilés-Barceló C (2012) Effect of amount of carbon nanotubes in polyurethane dispersions. Macromol Symp 321–322:135–139
22. Li G, Wang L, Ni H, Pittman CU (2001) Polyhedral oligomeric silsesquioxane (POSS) polymers and copolymers: a review. Inorg Organomet Polym 111:123–154
23. Su K, Bujalski DR, Eguchi K, Gordon GV, Hu S, Ou DL (2005) Vinyl ether-modified poly(hydrogen silsesquioxanes) as dielectric materials. J Mater Chem 15:4115–4124
24. Koh K, Sugiyama S, Morinaga T, Ohno K (2005) Precision synthesis of a fluorinated polyhedral oligomeric silsesquioxane-terminated polymer and surface characterization of its blend film with poly(methyl methacrylate). Macromolecules 38:1264–1270
25. Lai YS, Tsai CW, Yang HW, Wang GP, Wu KH (2009) Structural and electrochemical properties of polyurethanes/polyhedral oligomeric silsesquioxanes (PU/POSS) hybrid coatings on aluminum alloys. Mater Chem Phys 117:91–98
26. Bianchini D, Galland GB, Dos Santos JH (2005) Metallocene supported on a polyhedral oligomeric silsesquioxane-modified silica with high catalytic activity for ethylene polymerization. J Polym Sci Part A Polym Chem 43:5465–5476
27. McCusker C, Carroll JB, Rotello VM (2005) Cationic polyhedral oligomeric silsesquioxane (POSS) units as carriers for drug delivery processes. Chem Commun 8:996–998
28. Fu BX, Hsiao BS, Pagola S, Stephens P, White HM (2001) Structural development during deformation of polyurethane containing polyhedral oligomeric silsesquioxanes (POSS) molecules. Polymer 42:599–611
29. Bliznyuka VN, Tereshchenko TA, Gumenna MA (2008) Structure of segmented poly(ether urethane)s containing amino and hydroxyl functionalized polyhedral oligomeric silsesquioxanes (POSS). Polymer 49:2298–2305
30. Knight PT, Lee KM, Qin HH, Mather PT (2008) Biodegradable thermoplastic polyurethanes incorporating polyhedral oligosilsesquioxane. Biomacrom-molecules 9:2458–2467
31. Neumann D, Fisher M, Tran L, Matisons JG (2002) Synthesis and characterization of an isocyanate functionalized polyhedral oligosilsesquioxane and the subsequent formation of an organic−inorganic hybrid polyurethane. J Am Chem Soc 124:13998–13999
32. Liu H, Zheng S (2005) Polyurethane networks nanoreinforced by polyhedral oligomeric silsesquioxane. Macromol Rapid Commun 26:196–200
33. Turri S, Levi M (2005) Wettability of polyhedral oligomeric silsesquioxane nanostructured polymer surfaces. Macromol Rapid Commun 26:1233–1236
34. Turri S, Levi M (2005) Structure, dynamic properties, and surface behavior of nanostructured ionomeric polyurethanes from reactive polyhedral oligomeric silsesquioxanes. Macromolecules 38:5569–5574
35. Lee HT, Lin LH (2006) Waterborne polyurethane/clay nanocomposites: novel effects of the clay and its interlayer ions on the morphology and physical and electrical properties. Macromolecules 39:6133–6141
36. Oaten M, Choudhury NR (2005) Silsesquioxane−Urethane hybrid for thin film applications. Macromolecules 38:6392–6401
37. Raftopoulos KN, Koutsoumpis S, Jancia M, Lewicki JP, Kyriakos K, Mason HE, Harley SJ, Hebda E, Papadakis CM, Pielichowski K, Pissis P (2015) Reduced phase separation and slowing of dynamics in polyurethanes with three-dimensional POSS-based cross-linking moieties. Macromolecules 48:1429–1441
38. Yadav SK, Mahapatra SS, Ryu HJ, Yoo HJ, Cho JW (2014) Synthesis of high performance organic–inorganic composite via click coupling of block polymer and polyhedral oligomeric silsesquioxane. React Funct Polym 81:91–96

39. Zhang QC, Hu JK, Gong SL (2011) Preparation and characterization of aqueous polyurethane dispersions with well-defined soft segments. J Appl Polym Sci 122:3064–3070
40. Hu JK, Zhang QC, Gong SL (2012) Bridged polyhedral oligomeric silsesquioxane (POSS): a potential member of silsesquioxanes. Chin Chem Lett 23:181–184
41. Madbouly SA, Otaigbe JU (2009) Recent advances in synthesis, characterization and rheological properties of polyurethanes and POSS/polyurethane nanocomposites dispersions and films. Prog Polym Sci 34:1283–1332
42. Ash BJ, Schadler LS, Siegel RW (2004) Glass-transition temperature behavior of alumina/PMMA nanocomposites. J Polym Sci Part B Polym Phys 42:4371–4383
43. Rawal A, Urman K, Otaigbe JU, Schmidt-Rohr K (2006) Detection of nanometer-scale mixing in phosphate-glass/polyamide-6 hybrids by 1H–31P NMR. Chem Mater 18:6333–6338
44. Wang WS, Guo YL, Otaigbe JU (2009) The synthesis, characterization and biocompatibility of poly(ester urethane)/polyhedral oligomeric silesquioxane nanocomposites. Polymer 50:5749–5757
45. Wen J, Wikes GL (1996) Organic/inorganic hybrid network materials by the sol−gel approach. Chem Mater 8:1667–1681
46. Chang JH, An YU (2002) Nanocomposites of polyurethane with various organoclays: thermomechanical properties, morphology, and gas permeability. J Polym Sci Part B Polym Phys 40:670–677
47. Agag T, Koga T, Takeichi T (2001) Anticorrosively enhanced PMMA−clay nanocomposite materials with quaternary alkylphosphonium salt as an intercalating agent. Polymer 42:3393–3397